Conversion of α_1-Antichymotrypsin into a Human Neutrophil Elastase Inhibitor: Demonstration of Variants with Different Association Rate Constants, Stoichiometries of Inhibition, and Complex Stabilities†

Harvey Rubin,*,‡ Michael Plotnick,§ Zhi-mei Wang,‡ Xuzhuo Liu,‡ Qiuhui Zhong,‖ Norman M. Schechter,⊥ and Barry S. Cooperman‖

Department of Medicine and Microbiology, Pulmonary/Critical Care Division, Departments of Dermatology and of Biochemistry and Biophysics, and Department of Chemistry, University of Pennsylvania, Philadelphia, Pennsylvania 19104

Received January 3, 1994; Revised Manuscript Received March 22, 1994®

ABSTRACT: Despite the homology with α_1-protease inhibitor (α1PI), wild-type antichymotrypsin (ACT) is a substrate for HNE rather than an inhibitor of the enzyme. In order to investigate the nature of the specificity between serpins and serine proteases, the reactions of human neutrophil elastase (HNE) with wild-type recombinant ACT and recombinant variants of ACT were studied. ACT variants were generated where (1) the primary interaction site, the P1 position, was replaced with the P1 residue of α1PI, (2) the residues corresponding to P3–P3′ were replaced with those of α1PI, and (3) the residues corresponding to the canonical recognition sequence as well as flanking residues encompassing the exposed reactive loop of the inhibitor were replaced with the corresponding residues of α1PI. Each variant was analyzed to determine the effect of the replacements on reactions with human neutrophil elastase and chymotrypsin with regard to (1) the second-order rate constant for enzyme–serpin complex formation, (2) the number of moles of serpin required to completely inhibit 1 mol of enzyme (the stoichiometry of inhibition, SI), and (3) the stability of the enzyme–serpin complex. Replacing Leu with Met in the P1 position (rACT-L358M) was sufficient to convert rACT into an inhibitor of HNE with an apparent second-order rate constant ($k'/[I]$) of 4×10^4 M^{-1} s^{-1} and an SI of 5. The high SI was due to a concurrent hydrolytic reaction at sites in the reactive loop. N-Terminal sequence analysis of HNE cleavage products demonstrated a pattern similar to that of HNE cleavage of ACT, except that P1–P1′ cleavage was more highly represented in the rACT-L358M/HNE reaction. The complex of rACT-L358M and HNE was not long-lived, with return of almost complete enzyme activity in approximately 4 h. Replacement of six residues around the reactive center of ACT with those of α1PI (rACT-P3P3′) created an improved inhibitor of HNE. This variant had an apparent second-order rate constant of 1×10^5 M^{-1} s^{-1} and an SI of approximately 1. The HNE–rACT-P3P3′ complex demonstrated increased stability compared to rACT-L358M, with return of HNE activity occurring over a 20-h period. Larger loop switches of 15 and 20 residues resulted in variants (rACT-P10P5′ and rACT-P10P10′) that were substrates for HNE, hydrolyzed predominantly at P1–P1′ yet retained chymotrypsin inhibitory activity. These results suggest that the P1 position as well as residues surrounding this site are important for serpin function and specificity and that loop switches are not necessarily sufficient for transferring the structural elements responsible for biochemical activity.

The subfamily of serpins that inhibit serine proteases has characteristic properties that define their activity, i.e., the rate constant of complex formation (Travis & Salvesen, 1983), the stoichiometry of inhibition (SI)[1] (Rubin et al., 1990; Patston et al., 1991; Fish & Bjork, 1979), and the stability of the enzyme–serpin complex (Cooperman et al., 1993; Schechter et al., 1993; Padrines et al., 1989). At the present time, there is no general algorithm that describes the sequence of amino acids or structural motifs in serpins that are necessary and sufficient to explain these properties. It is generally held that the mechanism of inhibition involves a substratelike reaction between the serpin and enzyme where the enzyme stalls, possibly in a tetrahedral intermediate, thereby not completing hydrolysis of the reactive site: the P1–P1′ bond (Matheson et al., 1991; Travis & Carrell, 1985). This may be related to a conformational change in the serpin that occurs upon binding to the enzyme which in turn may induce a conformational change in the enzyme that disrupts the catalytic mechanism (Lawrence et al., 1990).

α1PI inhibits HNE with a second-order rate constant on the order of 10^7 M^{-1} s^{-1}, has a stoichiometry of inhibition of 1, and forms complexes that are stable for days (Padrines et al., 1989). Variants in the P1 position of α1PI, formed by replacing Met with Leu, Ile, Ala, or Val, inhibit HNE with slightly differing second-order rate constants, ranging from 2.4×10^6 to 6.7×10^6 M^{-1} s^{-1} (Jallat et al., 1986). On the other hand, ACT is not an inhibitor of HNE even though it contains Leu at the P1 site and is highly homologous to α1PI. In fact, HNE inactivates large molar excesses of ACT by cleavage at peptide bonds between reactive site residues at positions P4–P3 (Ile355-Thr356) and P1–P1′ (Leu358-

† This work was supported by funding from the NIH, Alexin Pharmaceuticals, and the Department of the Navy. Drs. Rubin, Schechter, Wang, and Cooperman have equity in Alexin.

* Correspondence should be addressed to the author at the University of Pennsylvania, School of Medicine, 536 Johnson Pavilion, 36th St. and Hamilton Walk, Philadelphia, PA 19104.

‡ Department of Medicine and Microbiology.

§ Pulmonary/Critical Care Division.

‖ Department of Chemistry.

⊥ Departments of Dermatology and of Biochemistry and Biophysics.

® Abstract published in *Advance ACS Abstracts,* May 15, 1994.

[1] Abbreviations: α1PI, α_1-protease inhibitor; ACT, antichymotrypsin; rACT, recombinant antichymotrypsin; HNE, human neutrophil elastase; SI, stoichiometry of inhibition; Chtr, Chymotrypsin.

0006-2960/94/0433-7627$04.50/0

Ser359) (Potempa et al., 1991). The difference in the reaction of HNE with α1PI and ACT suggests that having the "appropriate" P1 residue is not sufficient for inhibition and that additional constraints on the structure of the reactive loop are necessary. In this paper, we tested this proposition by replacing residues of the reactive loop of ACT with certain sets of residues derived from α1PI.

EXPERIMENTAL PROCEDURES

Materials. HNE and α1PI were obtained from CalBiochem. PMSF was obtained from Sigma. Standard proteins for SDS–PAGE gels were from BioRad or Enprotech. Peptide-nitroanilide substrates and *N*-MeO-Suc-AAPV-CMK were from Bachem. Chymotrypsin was from Sigma or Boehringer-Mannheim. Dodecyl maltoside was from Anatrace.

Determination of Inhibitor and Protease Concentrations. Recombinant inhibitors and α1PI concentrations were determined by active site titration using bovine chymotrypsin. Chymotrypsin concentrations were standardized by titration with the active site titrant *N-trans*-cinnamoylimidazole (Schonbaum et al., 1961). HNE concentrations were determined assuming a specific activity of 610 μmol of product min^{-1} (μmol of HNE)$^{-1}$, measured under standard conditions: 0.1 M Hepes, pH 7.5, 0.5 M NaCl, 9% Me_2SO_4, and 1 mM *N*-MeO-Suc-AAPV-*p*NA at 25 °C. The amount of *p*-nitroaniline formed was quantified using ϵ_{410} = 8800 M^{-1} cm^{-1}. To determine the specific activity, HNE concentrations were measured by active site titration with α1PI which was previously standardized against chymotrypsin.

Titrations and Time Course Studies. Titration reactions were performed in 50–100 μL containing 0.1 M Tris-HCl, pH 8.0, 0.1–0.4 M NaCl, and 0.01% dodecyl maltoside. The reaction mixture contained dodecyl maltoside to prevent nonspecific loss of HNE activity when the enzyme is present in low concentrations or in low salt; it has no effect on the specific activity of the enzyme (Schechter et al., 1993). HNE concentrations ranged between 150 and 400 nM. For titration experiments, incubations were usually for 15–30 min at 25 °C. Residual activity was measured by dilution of a sample aliquot in 1 mL of standard buffer so that initial hydrolytic rates of controls were between 0.4 and 0.75 Δabs/min. Substrate turnover was continuously monitored for 3 min in either a Beckman DU 65 or a Gilford 260 spectrophotometer. Rates of substrate hydrolysis remained constant over the 3-min monitoring time, indicating that the inhibitor–enzyme complexes were stable to dilution. Time course studies were performed similarly except that the reaction volume was increased to allow for repeated removal of reaction aliquots for measurement of residual activity as time progressed.

Determination of Inactivation Rate Constants. Rate constants were determined under pseudo-first-order conditions, $[I]_0 \gg [E]_0$, in the presence of substrate (0.5–1 mM) (Petersen & Clemmensen, 1981). Progress curves were monitored continuously for 10–15 min, and instantaneous velocities were determined for every 1-min interval. k_{obs}, the apparent rate constant in the presence of substrate, was determined by least-squares fitting of the velocity vs time data to an exponential, $V_0e^{-k_{obs}t}$, where V_0 is the initial velocity. The apparent rate constant was then corrected for substrate concentration according to the relationship: $k' = k_{obs}(K_m + [S])/K_m$ where k' is the product of the second-order rate constant and [I] (Schechter et al., 1993). The K_m of HNE for catalysis of *N*-MeO-Suc-AAPV-*p*NA was 0.15 mM in reactions containing 0.0–1.0 M NaCl, 0.09 M Hepes, pH 7.5, 0.01% dodecyl maltoside, and 9% DMSO. Second-order inactivation rate constants of α1PI with HNE and Chtr were determined at equimolar concentrations in the presence of substrate as described by Chmielewska et al. (1988) where $E_0 = I_0$, and k_{obs} was determined by fitting of velocity vs time data to the equation $V = V_0/(E_0k_{obs}t + 1)$. The apparent rate constant was then corrected for substrate concentration as above. The K_m of Chtr for catalysis of *N*-MeO-Suc-AAPL-*p*NA was 0.48 mM measured in reactions containing 0.0–1.0 M NaCl, 0.1 M Tris, pH 8.0, 0.01% dodecyl maltoside, and 9% DMSO.

SDS–PAGE Gel Electrophoresis. Reactions were stopped after 30 min by the addition of PMSF (final concentration 0.5 mM) or *N*-MeO-SuccAAPV-CMK (final concentration 0.1 mM). After an incubation period of 10 min, denaturing buffer including 2% SDS and 20 mM DTT (Laemmli, 1970) was added, and samples were heated at 90 °C for 10 min. Proteins were resolved on a 10–12% gel as described previously (Schechter et al., 1993) and visualized by staining with Coomassie Brilliant Blue.

N-Terminal Sequence Analysis of C-Terminal Peptides Released from the Reaction of HNE with ACT and ACT Variants. The C-terminal peptide fragment was isolated and sequenced as previously described (Schechter et al., 1989). Reaction conditions were set in Tris-HCl, pH 8.0, 0.1 M NaCl, and 0.01% dodecyl maltoside, such that less than 75% of the initial amount of ACT or ACT variant was cleaved or complexed by HNE. The products were resolved on a 17.5% SDS–polyacrylamide gel and electroblotted onto a PVDF membrane (Trans-Blot, BioRad), and bands were visualized by staining with Coomassie Blue R250. The 4-kDa band corresponding to the C-terminal peptide was excised and sequenced directly from the membrane at the protein chemistry facility of the Wistar Institute (Philadelphia) (Modzzanowski & Speicher, 1992; Reim & Speicher, 1992). Recovery of the C-terminal peptide was approximately 5–10%.

Construction, Expression, and Purification of Variant rACT's. The construction of the ACT expression vector pACT and the purification of recombinant ACT have been described previously (Rubin et al., 1990). Construction of the cassette vector is as described in Kilpatrick et al. (1991). Briefly, starting with pACT and using standard site-directed mutagenesis, a unique *Kpn*I restriction site was created at the position corresponding to P10–P9, changing Ala-Ala to Gly-Thr, and an *Mlu*I restriction site was created at P10′–P11′, changing Val to Thr. The association rate constant of the variant rACT encoded by this expression vector is 5×10^6 M^{-1} s^{-1} and has a reaction stoichiometry of 1. Cassette variants were then created by removing the *Kpn*I–*Mlu*I fragment and inserting a synthetic double-stranded oligonucleotide of predesigned coding sequences. The rACT-P3P3′ and rACT-P10P10′ variants were generated in the cassette vector. rACT-P10P5′ was prepared in the cassette vector which contains an Ala at the P10′ position arising from a specific restriction site engineered into an expression vector prepared earlier. rACT-L358M was generated by site-directed mutagenesis of rACT (Rubin et al., 1990). A second rACT-P3P3′ variant without the P10–P9 and P10′–P11′ changes was prepared using an overlap extension PCR method (Ho et al., 1989). This variant was used for the N-terminal analysis after reaction with HNE. No significant difference was noted in the rate of inhibition, $[I]_0/[E]_0$, or stability of the complex between the two rACT-P3P3′ variants. The reactive loop sequences of the ACT variants, wild-type ACT and α1PI, are shown in Figure 1.

RESULTS

Reaction of rACT with HNE. HNE completely inactivated a greater than 100-fold excess of rACT, demonstrating the

Table 1: Amino-Terminal Sequences of the 4-kDa Fragment of ACT and Variants Digested with HNE[a]

inhibitor	cycle 1	2	3	4	5	6	7	8	9	10
rACT	T(13)	L(28)	L(28)	S(5)	A(18)	L(18)	V(14)	E(18)	T(7)	R(10)
	K(13)	I(8)	T(5)	L(10)	L(10)	S(3)	A(8)	L(8)	V(4)	E(7)
	S(3)	A(4)	L(*)[b]	V(3)	E(3)	T(2)	R(3)	T(2)	I(2)	V(1)
rACT-L358M[c]	T(13)	L(35)	M(31)	S(5)	A(27)	L(24)	V(20)	E(23)	T(8)	R(8)
	S(5)	A(20)	L(20)	V(16)	E(18)	T(8)	R(12)	T(5)	I(10)	V(12)
	K(16)	I(14)	T(9)	L(20)	M(17)	S(2)	A(15)	L(16)	V(16)	E(12)
rACT-P3P3′	S(8)	I(19)	P(23)	V(16)	E(18)	T(5)	R(11)	T(4)	I(6)	V(5)
	K(3)	I(*)	I(*)	P(*)	M(4)	S(1)	I(2)	P(2)	V(*)	E(1)
rACT-P10P5′	S(22)	I(47)	P(75)	P(62)	E(59)	T(23)	R(42)	T(22)	I(33)	A(49)

[a] Numbers in parentheses denote picomoles recovered. [b] An asterisk denotes that the yield of this residue for this sequence is difficult to assign due to the same residue in overlapping sequences. [c] Several sequences starting with residues on the C-terminal side of P1–P1′ were detected for rACT-L358M and rACT-P10P5′ in the <5 pmol range. These were thought to be the result of secondary cleavages.

INHIBITOR	REACTIVE LOOP
	P10 P1 P10′
ACT	SAATAVKITLLSALVETRTIVRFN
rACT-L358M	M
rACT-P3P3′	GT IPMSIP T
rACT-P3P3′(no cassette)	IPMSIP
rACT-P10P10′	GTMFLEAIPMSIPPEVKFNT
rACT-P10P5′	GTMFLEAIPMSIPPE A
α1PI	AGAMFLEAIPMSIPPEVKFNKPFT

FIGURE 1: Reactive loop sequences of serpins and variants.

substrate nature of the interaction. N-Terminal sequence analysis of the small cleavage products (approximately 4 kDa) demonstrated hydrolysis primarily at positions P4–P3 (Ile355-Thr356) and P6–P5 (Val353-Lys354) with very little at P1–P1 (Leu358-Ser359) (Table 1). SDS gel analysis of the reaction products showed a faint band at a position consistent with that expected for rACT–HNE complexes. The presence of this product may suggest the formation of a short-lived inhibitory complex.

We produced a series of variant rACT's, generated by placing progressively larger segments of the reactive loop of α1PI in the equivalent regions in ACT, in order to structure to define the sequence conditions under which ACT could be converted into an inhibitor of HNE. All variants inhibited bovine pancreatic chymotrypsin (Table 2), indicating that they were well folded. Titration with chymotrypsin was used to determine inhibitor concentrations for all variants except for rACT-P10P10 and rACT-P10P5′, for which concentrations were determined by protein measurement.

Reaction of rACT-L358M with HNE. The reaction of HNE with rACT-L358M was significantly different from that with wild-type ACT. This variant inhibited HNE activity with an apparent second-order rate constant ($k'/[I]$) of 4×10^4 M^{-1} s^{-1} (Table 2). Titration experiments demonstrated that complete inhibition of HNE was achieved at an $[I]_0/[E]_0$ value of 5 (Figure 2A). A variety of species were generated when rACT-L358M was incubated with varying concentrations of HNE as shown by SDS–PAGE analysis (Figure 3). When $[I]_0 = [E]_0$, three major species were detected: one at M_r 68 000 corresponding to one form of the enzyme–inhibitor complex (C), one corresponding to a degraded form of the inhibitor (DI-2), and one corresponding to intact HNE. As $[I]_0/[E]_0$ increased, two other bands became visible corresponding to slightly higher molecular weight forms of both the complex and the degraded inhibition

Table 2: Kinetic Parameters for the Reaction of Chymotrypsin and Human Neutrophil Elastase with rACTs and α1PI

inhibitor	Chtr	HNE
	$k'/[I]$[a] ($\times 10^{-4}$ M^{-1} s^{-1})	
rACT[b]	100	substrate
rACT-P10P10′	3.3	substrate
rACT-P10P5′	4.0	substrate
rACT-L358M[b]	30	4
rACT-P3P3′	1.8	10
α1PI[c]	600	5000
	SI	
rACT	1	
rACT-P10P10′	3.0	
rACT-P10P5′	3.5	
rACT-L358M	1	5
rACT-P3P3′	1	1.4
α1PI[c]	1	1

[a] Inhibition rate constants determined under pseudo-first-order conditions, $[I]_0 \gg [E]_0$, and at least 18–15-fold higher than the SI. [b] Taken from Rubin et al. (1990). [c] Taken from Beatty et al.

(DI). Finally, undegraded inhibitor (UI) was visible at an $[I]_0/[E]_0$ of 5 or greater, and the band corresponding to HNE was absent, consistent with the titration results. N-Terminal amino acid sequence analysis of the 4-kDa fragments released on incubation of rACT-L358M with HNE (at $[I]_0/[E]_0$ approximately 10) showed that cleavage in the reactive loop occurred primarily at position P4–P3 (Ile-Thr) followed quantitatively by cleavage at P6–P5 (Val-Lys) and P1–P1′ (Met-Ser) (Table 1). However, cleavage at the P1–P1′ position made up a significantly greater proportion of the products found with the HNE–rACT-L358M interaction than with HNE–rACT. We previously estimated the second-order rate constant for inhibition of HNE by rACT-L358M as $<10^3$ M^{-1} s^{-1} (Rubin et al., 1990). This estimate was derived from studies using equimolar concentrations of the variant inhibitor and HNE, where reaction stoichiometries of greater than 1 made it difficult to observe a measurable rate of inhibition.

At all $[I]_0/[E]_0$, the initial rapid loss in HNE activity was followed by a return of activity over a period of hours at both high (0.4 M) and low (0.1 M) [NaCl] (Figure 2B,C). The rate of return was considerably increased at the higher ionic strength.

Reaction of rACT-P3P3′ with HNE and Chtr. The variant that contains six residues from α1PI (IPMSIP) in the P3–P3′ positions of ACT, rACT-P3P3′, inhibited HNE with an apparent second-order rate constant of 1.1×10^5 M^{-1} s^{-1} (Table 2).

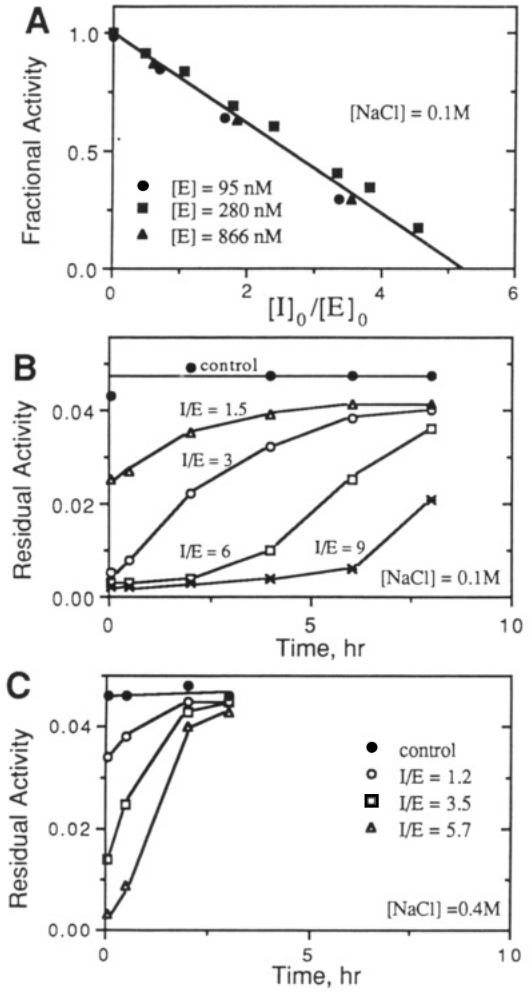

FIGURE 2: (A) Titration of HNE with rACT-L358M in 0.1 M NaCl. Residual activities in titrations were determined after a 15-min incubation. The same SI was obtained for HNE concentrations of 95, 280, and 866 nM. (B) Time course of HNE release from rACT-L358M–HNE complexes at different I/E ratios in 0.1 M NaCl and in (C) 0.4 M NaCl. The concentration of HNE in the time course experiments was 450 nM.

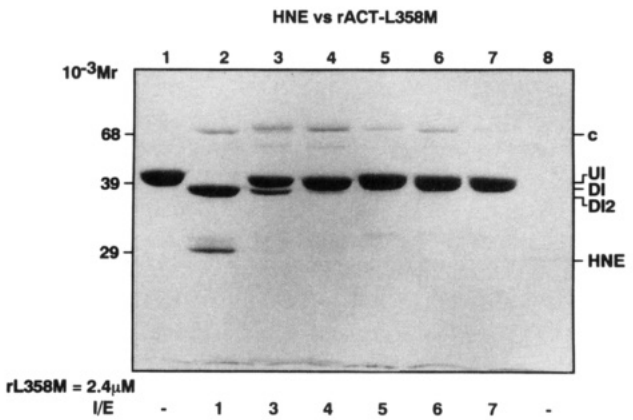

FIGURE 3: SDS–PAGE analysis of titration of HNE and rACT-L358M. Lane 1, rACT-L358M; lane 2, rACT-L358M reacted for 10 min with active HNE at $[I]_0/[E]_0 = 1$ followed by excess *N*-MeO-Suc-AAPV-CMK; lane 3, $[I]_0/[E]_0 = 3$; lane 4, $[I]_0/[E]_0 = 4$; lane 5, $[I]_0/[E]_0 = 5$; lane 6, $[I]_0/[E]_0 = 6$; lane 7, $[I]_0/[E]_0 = 7$; lane 8, HNE. C, UI, DI, and DI-2 represent complex, undegraded inhibitor, and degraded inhibitor primary and secondary cleavage products, respectively. The gel was run under reducing conditions.

An $[I]_0/[E]_0$ ratio of 1.4 was sufficient to produce complete inhibition of HNE as shown in titration studies (Figure 4A). SDS gel analysis (Figure 5) clearly showed high molecular

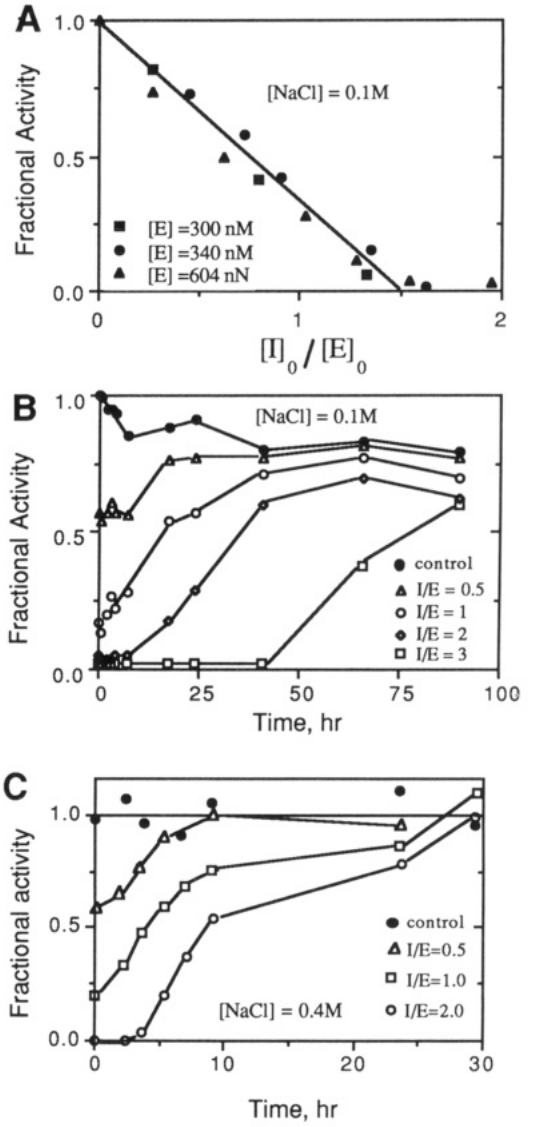

FIGURE 4: (A) Titration of HNE with rACT-P3P3′ in 0.1 M NaCl. Residual activity was measured after a 15-min incubation period. (B) Time course of release of HNE from rACT-P3P3′–HNE complex at different $[I]_0/[E]_0$ ratios in 0.1 M NaCl and in (C) 0.4 M NaCl.

weight bands corresponding to complex formation between rACT-P3P3′ and HNE. At $[I]_0/[E]_0 = 1$, i.e., when the stoichiometry of reactants was not sufficient to completely inhibit the enzyme, bands corresponding to degraded inhibitor and degraded inhibitor–enzyme complexes were visible on the gel. The presence of bands corresponding to undegraded inhibitor and enzyme–inhibitor complex seen when $[I]_0/[E]_0 = 2$ or 4 is consistent with the titration that showed an SI of 1.4. Bands corresponding to complexes of intermediate sizes, also seen in these lanes, may arise from HNE-dependent proteolysis of the HNE–rACT-P3P3′ complex, given that both free HNE and the complex will be present simultaneously in solution prior to completion of the complexation reaction. N-Terminal analysis of the 4-kDa reaction products demonstrated that the dominant interaction occurred through the P1–P1′ site with very small amounts arising from the P6–P5 position (Table 1).

The HNE–rACT-P3P3′ complex was significantly more stable than the HNE complex with rACT-L358M (cf. Figures 3B,C and 4B,C).

Of the three characteristics of serpin/protease interaction, association rate, stoichiometry of inhibition, and complex

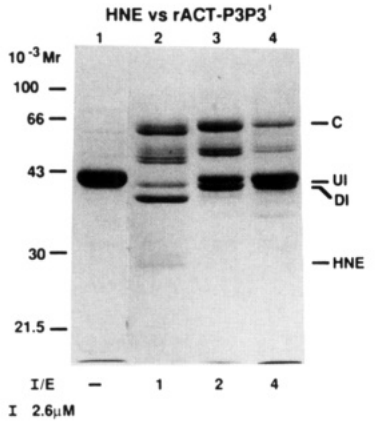

FIGURE 5: SDS–PAGE analysis of reaction products of HNE and rACT-P3P3′ after 30-min incubation in buffer containing 0.1 M NaCl. Lane 1, unreacted rACT-P3P3′; lanes 2–4, rACT-P3P3′ reacted with increasing concentrations of HNE with $[I]_0/[E]_0$ shown under the lane. The complexity of the pattern in lane 2 presumably reflects degradation of the HNE–rACT-P3P3′ complex by free HNE (2). At higher $[I]_0/[E]_0$, no free HNE is present. $[I]_0$ was 2.6 μM. The gel was run under reducing conditions.

stability, rACT-P3P3′ achieved almost maximal efficiency as an inhibitor, i.e., a low stoichiometry and a relatively stable complex. However, the second-order rate constant was 2 orders of magnitude lower than that of α1PI with HNE. In order to test whether this lower rate could be due to less favorable electrostatic interactions between rACT-P3P3′ and HNE as compared with α1PI and HNE, the second-order rate constants for these two reactions were measured as a function of ionic strength. Similar inhibitory effects of increasing salt on both interactions indicated differential electrostatic interactions were not the cause of the slower rate constant. The ionic strength dependence of the interaction of rACT-P3P3′ and α1PI with Chtr was also comparable.

Reaction of rACT-P10P5′ and rACT-P1010′ with HNE and Chtr. These rACT variants showed no stable inhibition of HNE, even at high $[I]_0/[E]_0$ (Figure 6A). In contrast, rACT-P10P10′ formed SDS-stable complexes with chymotrypsin (Figure 7), albeit with an SI of 3 (Figure 6B). Another variant containing an extended loop substitution, but a shorter "prime side" replacement, rACT-P10P5′, inhibited Chtr and was also a slow substrate for HNE (data not shown). N-Terminal analysis of the HNE–rACT-P10P5′ interaction demonstrated cleavage primarily of the P1–P1′ (Met358-Ser359) bond. There was no evidence for P6–P5 and P4–P3 cleavages.

DISCUSSION

The reactive loop of rACT is a substrate for ACT because it contains major cleavage sites at P6–P5 and P4–P3 and a minor site at P1–P1′. The relatively conservation replacement of Leu358 to Met358 converted rACT into an inhibitor of HNE, albeit with an SI of 5. Leu and Met are recognized by the S1 subsite of HNE approximately equally when presented to the enzyme as single-site mutations of α1PI (Jallat et al., 1986), suggesting that improved binding specifically at this site was not responsible for the greater interaction of the rACT-L358M variant with HNE and conversion from substrate to inhibitor. Rather, we suggest that the Leu to Met replacement altered the reactive loop so as to allow for a more easily attained canonical inhibitory conformation and that additional structural constraints could be imposed on the loop such that hydrolysis could be completely suppressed via facile generation of a "canonical inhibitory" sequence. This

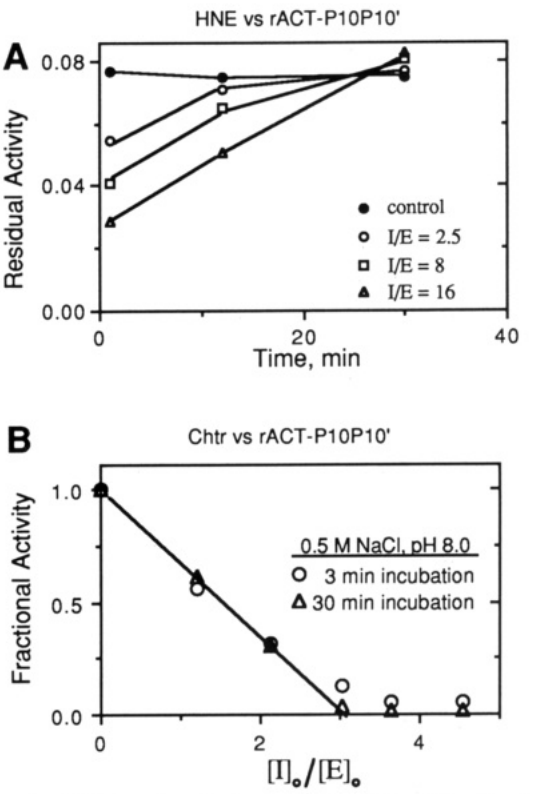

FIGURE 6: (A) Titration of chymotrypsin (240 μM) with rACT-P10P10′ in 0.5 M NaCl/0.01 M Tris-HCl (pH 8.0). (B) Time course of HNE activity after incubation with rACT-P10P10′ at different $[I]_0/[E]_0$ ratios in 0.1 M NaCl.

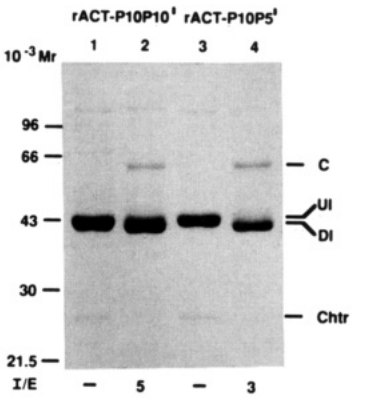

FIGURE 7: SDS–PAGE analysis of the reaction of rACT-P10P10′ and rACT-P10P5′ with Chtr. rACT-P10P10′ (lane 1) and rACT-P10P10′ reacted with chymotrypsin (lane 2); rACT-P10P5′ (lane 3) and rACT-P10P5′ reacted with chymotrypsin (lane 4). Reaction buffers contained 0.1 M NaCl. UI and DI represent undegraded inhibitor and degraded inhibitor, respectively. Gels were run under nonreducing conditions.

suggestion was supported by the results of the interaction of HNE with the ACT variant in which the P3–P3′ residues were replaced by the P3–P3′ residues of α1PI. This inhibitor had a stoichiometry of inhibition of 1.4, yet the primary substrate sites (P6–P5 and P4–P3) remained in the loop. N-Terminal sequence analysis of the reaction products confirmed the dominance of the P1–P1′ interaction with the enzyme, suppression of P4–P3 cleavage, and only a very minor cleavage reaction at P6–P5. While the P3 residue was altered from Thr to Ile in the construction of rACT-P3P3′, it is unlikely that this substantially reduced cleavage of the P4–P3 bond given the known HNE cleavage preferences (Bode et al., 1989) and other serpin cleavage products generated by HNE (Carrell et al., 1985).

We also tested the hypothesis that altering the rate at which strand 4A insertion into the A β sheets might change the SI of the reaction of the serpin with HNE by extending the loop substitutions to include residues that should not be able to completely insert into the A sheet of ACT. Modeling studies and experiments with synthetic peptides (Schulze et al., 1990) strongly suggest that the P1–P10 residues of the rACT-P10P10′ and rACT-P10P5′ variants, which were derived from the α1PI sequence, should not insert as efficiently as the wild-type residues because of unfavorable interactions between the β sheet of ACT and large hydrophobic residues, M, F, and L at positions P8, P7, and P6, respectively, in the variant 4A strand. Analysis of guanidine hydrochloride denaturation of the cleaved form of both rACT-P10P10′ and rACT-P10P5′ using circular dichroism spectroscopy is consistent with only partial insertion of strand 4A (J. Zhong, unpublished results). These variants showed no stable inhibition of HNE, even at high $[I]_0/[E]_0$ stoichiometries. N-Terminal analysis of the reaction products was consistent with a primary substrate reaction through the P1–P1′ site. In contrast, rACT-P10P10′ and rACT-P10-P5′ inhibited and formed SDS-stable complexes with Chtr, each with an SI of approximately 3. While it is possible that the SI of 3 represents partially unfolded protein that undergoes partitioning, it is unlikely given that the specific cleavage site at P1–P1′ was observed. These results are consistent with the strand insertion criterion for inhibitors with an additional requirement that sufficient strand insertion must occur prior to, or faster than, the hydrolytic reaction in the reaction loop. The examples of the large loop substitutions described above suggest that HNE cleaves these loops faster than strand insertion whereas cleavage of the loop by Chtr occurs on a time scale comparable to strand insertion. A similar result has recently been reported with antithrombin III where a mutant in which the P10–P10′ region was altered lost inhibitory activity while a P3–P3′ variant demonstrated almost full inhibitory activity (Theunissen et al., 1993).

Analyses of the reaction of serpins with target serine proteases based on the rate constant for complex formation, the reaction stoichiometry, and the stability of the complex offer a powerful methodology with which to investigate well-defined characteristics of the enzyme–inhibitor interaction as well as to correlate biological consequences with biochemical properties of the reaction. For example, consideration of the rate constant for complex formation has led to descriptions of acquired and hereditary serpin deficiencies causing diseases of the lung, and abnormalities of the coagulation and the fibrinolytic systems [reviewed in Gettins et al. (1992)]. Recently, the importance of the stoichiometry of the reaction has been recognized with the discovery that cleaved inhibitors, as well as the enzyme–inhibitor complexes, induce IL6 production (Kurdowska & Travis, 1990) and are chemoattractants (Potempa et al., 1991; Banda et al., 1988a,b; Hofmann et al., 1989). In addition, the ACT–Chtr complex is a chemoattractant (Banda et al., 1988a,b) and inhibits the production of free radicals by activated neutrophils (Schuster et al., 1992). The ability to create serpin variants that have specific reaction properties will now allow us to analyze the mechanisms associated with these properties and could be the basis of important new therapeutic agents.

ACKNOWLEDGMENT

We thank Linda Jordan, April James, Pirjo Tuominen, Nora Zuno, and Lisa Benke for excellent technical assistance.

REFERENCES

Banda, M. J. Rice, A. G., Griffin, G. L., & Senior, R. M. (1988a) *J. Biol. Chem. 263*, 4481–4484.
Banda, M. J. Rice, A. G., Griffin, G. L., & Senior, R. M. (1988b) *J. Exp. Med. 167*, 1608–1615.
Beatty, K., Bieth, J., & Travis, J. (1980) *J. Biol. Chem. 255*, 3931–3934.
Bjork, I., Nordling, K., Larsson, I., & Olson, S. T. (1992) *J. Biol. Chem. 267*, 19047–19050.
Bode, W., & Huber, R. (1991) *Curr. Opin. Struct. Biol. 1*, 45–52.
Bode, W., Meyer, E., & Powers, J. C. (1989) *Biochemistry 28*, 1951–1963.
Carrell, R. W., & Owen, M. C. (1985) *Nature 317*, 730–732.
Carrell, R. W., Evans, D. L., & Stein, P. E. (1991) *Nature 353*, 576–578.
Chmielewska, J., Ranby, M., & Wiman, B. (1988) *Biochem. J. 251*, 327–332.
Cooperman, B. S., Nickbarg, E., Stavridi, E., Rescorla, E., Schechter, N., & Rubin, H. (1993) *J. Biol. Chem.*, 23616–23625.
Declerck, P. J., De Mol, M., Vaughan, D. E., & Collen, D. (1992) *J. Biol. Chem. 267*, 11693–11696.
Fish, W. W., Orre, K., & Bjork, I. (1979) *FEBS Lett. 98*, 103–106.
Gettins, P., Patston, P. A., & Schapira, M. (1992) *Hematol. Oncol. Clin. N. A. 6*, 1393–1409.
Ho, S. N., Hunt, H. D., Horton, R. M., Pullen, J. K., & Pease, L. R. (1989) *Gene 77*, 51–59.
Hoffman, M., Pratt, C. W., Brown, R. L., & Church, F. C. (1989) *Blood 73*, 1682–1685.
Hubbard, S. J., Campbell, S. F., & Thorton, J. M. (1991) *J. Mol. Biol. 220*, 507–530.
Jallat, S., Caravallo, D., Tessier, L. H., Roecklin, D., Roitsch, C., Ogushi, F., Crystal, R. G., & Courtney, M. (1986) *Protein Eng. 1*, 29–35.
Kilpatrick, L., Johnson, J. L., Clifford, T. F., Banach, M., Cooperman, B. S., Douglas, S. D., & Rubin, H. (1991) *J. Immunol. 146*, 2388–2393.
Kurdowska, A., & Travisd, J. (1990) *J. Biol. Chem. 265*, 21023–21026.
Laemmli, U. K. (1970) *Nature 227*, 680–685.
Lawrence, D. A., Strandberg, L., Ericson, J., & Ny, T. (1990) *J. Biol. Chem. 265*, 20293–20301.
Matheson, N. R., Van Halbeek, H., & Travis, J. (1991) *J. Biol. Chem. 266*, 13489–13491.
Modzzanowski, J., & Speicher, D. W. (1992) *Anal. Biochem. 207*, 11–18.
Padrines, M., Schneider-Pozzer, M., & Bieth, J. G. (1989) *Am. Rev. Respir. Dis. 139*, 783–790.
Patston, P. A., Gettins, P., Beechem, J., & Schapira, M. (1991) *Biochemistry 30*, 8876–8882.
Petersen, L. C., & Clemmensen, I. (1981) *Biochem. J. 199*, 121–127.
Potempa, J., Fedak, D., Dubin, A., Mast, A., & Travis, J. (1991) *J. Biol. Chem. 266*, 21482–21487.
Pratt, C. W., Tobin, R. B., & Church, F. C. (1990) *J. Biol. Chem. 265*, 6092–6097.
Reim, D. F., & Speicher, D. W. (1992) *Anal. Biochem. 207*, 19–23.
Rubin, H., Wang, Z. M., Nickbarg, E. B., McLarney, S., Naidoo, N., Schoenberger, O. L., Johnson, J. L., & Cooperman, B. S. (1990) *J. Biol. Chem. 265*, 1199–1207.
Schechter, N. M., Sprows, J. L., Schoenberger, O. L., Lazarus, G. S., Cooperman, B. S., & Rubin, H. (1989) *J. Biol. Chem. 264*, 21308–21315.
Schechter, N. M., Jordan, L. M., James, A. M., Cooperman, B. S., Wang, Z.-M., & Rubin, H. (1993) *J. Biol. Chem.* 23626–23633.

Schonbaum, G. R., Zerner, B., & Bender, M. L. (1961) *J. Biol. Chem.*, 2930–2935.

Schulze, A. J., Baumann, U., Knof, S., Jaeger, E., Huber, R., & Laurell, C.-B. (1990) *Eur. J. Biochem. 194*, 51–56.

Schuster, M., Enriquez, P. M., Curran, P., Cooperman, B. S., & Rubin, H. (1992) *J. Biol. Chem. 267*, 5056–5059.

Skriver, K., Wikoff, W. R., Patston, P. A., Tausk, F., Schapira, M., Kaplan, A. P., & Bock, S. C. (1992) *J. Biol. Chem. 266*, 9216–9221.

Stein, P. E., Leslie, A. G. W., Finch, J. T., Turnell, W. G., McLaughlin, P. J., & Carrell, R. W. (1990) *Nature 347*, 99–102.

Theunissen, H. J. M., Dijkema, R., Grootenhuis, P. D. J., Swinkels, J. C., de Poorter, T. L., Carati, P., & Visser, A. (1993) *J. Biol. Chem. 268*, 9035–9040.

Travis, J., & Salvesen, G. S. (1983) *Annu. Rev. Biochem. 52*, 655–709.

Travis, J., & Carrell, R. (1985) *Trends Biochem. Sci. (Pers. Ed.) 10*, 20–24.